NASA TM X-79

TECHNICAL MEMORANDUM

X - 79

AN EXPERIMENTAL INVESTIGATION OF AERODYNAMIC EFFECTS OF AIRFOIL THICKNESS ON TRANSONIC FLUTTER CHARACTERISTICS

By Robert V. Doggett, Jr., A. Gerald Rainey,
and Homer G. Morgan

Langley Research Center
Langley Field, Va.

NATIONAL AERONAUTICS AND SPACE ADMINISTRATION
WASHINGTON November 1959

NATIONAL AERONAUTICS AND SPACE ADMINISTRATION

TECHNICAL MEMORANDUM X-79

AN EXPERIMENTAL INVESTIGATION OF AERODYNAMIC EFFECTS OF AIRFOIL THICKNESS ON TRANSONIC FLUTTER CHARACTERISTICS*

By Robert V. Doggett, Jr., A. Gerald Rainey, and Homer G. Morgan

SUMMARY

An experimental investigation was made of the aerodynamic effects of airfoil thickness on the transonic flutter characteristics of two types of wings. The first type of wing had a rectangular, unswept plan form with circular-arc airfoil sections. The second type of wing had a swept, tapered plan form with NACA 65A-series airfoil sections. For each type of wing, different models having similar mass and stiffness properties were tested at Mach numbers from about 0.70 to 1.10. Within the range covered, it was found that an increase in airfoil thickness had a stabilizing effect in that higher fluid density was required to produce flutter at a given Mach number.

author

INTRODUCTION

Although present-day aircraft are being designed to operate at high supersonic speeds and the aeroelastician has begun to devote much of his attention to flutter at these and higher Mach numbers, fundamental knowledge of the factors which affect transonic flutter characteristics has also become of increasing importance since traversal of this range is necessary in reaching the higher speeds. It has generally been assumed that at transonic speeds, aerodynamic effects of such properties as airfoil shape, airfoil thickness, Reynolds number, and so forth on flutter characteristics are small, but this assumption has continually been of concern. Since there exists no complete analytical method by which the effects of the foregoing parameters may be predicted, the aircraft designer must of necessity look to experimental results for information on these effects. In this investigation one of these factors, namely,

*Title, Unclassified.

the aerodynamic effects of airfoil thickness on transonic flutter characteristics, is considered. For high subsonic speeds some information is available on the oscillatory lift and moment derivatives as a function of airfoil thickness (ref. 1), and some low-speed wind-tunnel test results are available on the effects of airfoil thickness on flutter characteristics (ref. 2), but transonic flutter data on the effect of airfoil thickness are meager or nonexistent.

In the present investigation, studies were made of the aerodynamic effects of airfoil thickness on the transonic flutter characteristics of two types of wings. The first type of wing had a rectangular, unswept plan form with circular-arc airfoil sections. This plan form was chosen in order to facilitate comparisons of the results with theory. Flutter calculations were made for the unswept wings at subsonic, sonic, and supersonic speeds. The second type of wing was a more practical configuration, having 45° of sweepback, a taper ratio of 1/7, and NACA 65A-series airfoil sections. For each type of wing, different models having various thickness ratios but with nearly the same mass and stiffness characteristics were tested in the Langley 2-foot transonic aeroelasticity tunnel in the Mach number range from about 0.70 to 1.10.

SYMBOLS

a	speed of sound, ft/sec
b	model semichord measured parallel to root at three-quarter span station, ft
EI	model bending stiffness, lb-in.^{2}
GJ	model torsion stiffness, lb-in.^{2}
g	structural damping coefficient
I_α	torsional moment of inertia per unit span, ft-lb-sec^2/ft
k_f	reduced frequency, $b\omega_f/V$
M	Mach number
m	total mass, slugs
m_l	mass per unit length, slugs/ft

q	dynamic pressure, $\frac{1}{2}\rho V^2$, lb/sq ft
R	Reynolds number based on model reference chord 2b
V	stream velocity, ft/sec
μ	mass-ratio parameter (see section entitled "Results and Discussion")
$\Lambda_{c/4}$	angle of sweepback of quarter-chord line, deg
ρ	density, slugs/cu ft
ω	circular frequency, radians/sec

Subscripts:

f	values at flutter
h, n	bending mode, n = 1, 2
α	torsion mode

APPARATUS AND PROCEDURE

Wind Tunnel

The investigation was conducted in the Langley 2-foot transonic aeroelasticity tunnel. This tunnel is a slotted-throat single-return wind tunnel equipped to use either air or Freon-12 as the test medium at pressures from 1 atmosphere down to about 1/25 atmosphere. The present tests were made with Freon-12 as the test medium. The tunnel is of the continuous-operation type and is powered by a motor-driven fan. Both test-section Mach number and density are continuously controllable.

Models

Two different types of semispan, cantilever-mounted wing models were tested. The first type consisted of a series of four rectangular, unswept wing models with circular-arc airfoil sections. These models had ratios of thickness to chord equal to 4, 6, 8, and 10 percent and are referred to as the unswept series. The second type was composed of a series of four tapered, sweptback-wing models with NACA 65A-series airfoil sections of 2-, 4-, 6-, and 8-percent thicknesses, and these models

are referred to as the swept series. Also included in each series was a 0.065-inch-thick aluminum-alloy flat plate having the same plan form as the models with varying thicknesses. Both the leading and trailing edges of these flat plates were beveled. All of the models of both series, including the flat plates, were equipped with two sets of resistance-wire strain-gage bridges arranged to be sensitive to bending and torsion, respectively. All of the models were rigidly clamped at the root, and the type of clamping used was identical in all cases. The geometry of the models of each series is presented in figure 1. Since it was necessary to have the physical properties of the models of each series as similar as possible and yet vary the model thickness, the models were constructed in such a way that the stiffness and mass were concentrated in a metal insert which was then covered with a light, flexible material which gave the desired airfoil shape.

For the unswept-wing models a 0.065-inch-thick aluminum-alloy insert of the desired plan form was covered with a lightweight flexible plastic foam. The aluminum insert determined the bending and torsional stiffnesses, elastic axis location, mass, and mass distribution of the model. A 2-inch spanwise section of the insert was left uncovered at the root to provide space for the model to be attached to the tunnel in mounting blocks. For the models of this series the foam added comparatively little mass and stiffness to that of the aluminum-alloy spar. The properties of the unswept models are presented in table I(a) and figures 2 and 3. The bending rigidity and torsional rigidity of the models were determined experimentally from the static deflection curves of the wings in bending and torsion. The structural damping coefficients for each of the models were obtained from decrements in still air. The node lines for the second bending and first torsion modes were determined from time-exposure photographs of the models oscillating in these modes. After the tunnel tests the models were segmented into 10 spanwise sections, and the mass, the center-of-gravity location, and the torsional moment of inertia were determined for each of these sections.

The swept-wing models were also constructed by covering a 0.065-inch-thick aluminum-alloy insert of the desired plan form with a lightweight flexible plastic foam. However, in this series the addition of the foam had more of an effect on the model properties than in the unswept series. This effect is seen in table I(b), where the model properties for the swept series are presented, and in figure 3, where some representative model parameters are plotted against percent thickness for the models of each series. As is seen in the figure, the unswept models exhibit a high degree of similarity; in the case of the swept wings, however, the degree of similarity is not so good. There is good agreement between the swept models only in regard to frequency but poor agreement in regard to mass and structural damping coefficient.

The node lines for the second and third natural modes for the swept models are presented in figure 2. These node lines were determined by observing the locus of points of no vibration of grains of sand placed on the models while they were oscillating in their respective modes. Given in table II are the normalized mode shapes for the first three natural modes of the 2-percent-thick swept model. These mode shapes were determined by a photographic technique similar to the one described in reference 3 and are believed to be typical of the modes for all of the models in this series.

Test Procedure

The same general procedure was used for all the tests. The determination of a typical flutter point proceeded as follows: With the tunnel evacuated to a low stagnation pressure, the compressor speed was increased until the desired test-section Mach number was reached. With the compressor speed held constant, the test-section Mach number was held nearly constant, and the test-section density was gradually increased by bleeding Freon-12 into the tunnel through an expansion valve until flutter was reached. The test-section dynamic pressure and Mach number were then rapidly decreased by actuating a "flutter stopper" (a spoiler in the diffuser section of the tunnel). The actuation of the flutter stopper also locked the tunnel instruments so that the tunnel conditions necessary to completely describe the flutter point could be recorded after precautions had been taken to save the model. The compressor speed was then decreased to a point well below the flutter condition and the spoiler was retracted. At this time the tunnel density was increased by a small amount, after which the test-section Mach number was slowly increased until the next flutter condition occurred. This same type of procedure was repeated several times, completely defining the flutter region within the operational limits of the tunnel.

During each flutter condition the outputs from the bending and torsion resistance-wire strain gages mounted near the model root were recorded on a recording oscillograph. From these oscillograph records the flutter frequencies were determined. The first three natural frequencies and the corresponding structural damping coefficients were obtained for each model before and after each tunnel test to determine whether or not the model had been damaged.

RESULTS AND DISCUSSION

The basic data obtained are presented in table III and in figure 4. The curves shown in figure 4 represent stability boundaries in terms of the variation with Mach number of the altitude-stiffness parameter

$\frac{b\omega_\alpha}{a}\sqrt{\mu}$. The altitude-stiffness parameter depends upon the physical properties of the wing; in particular, the torsional stiffness, and upon the atmosphere in which the wing operates. The value of this parameter increases as either altitude or stiffness increases. When plotted as the ordinate against Mach number, curves for constant dynamic pressure will appear as radial lines through the origin. The stable region is above the boundary. For the unswept models the mass-ratio parameter μ is defined as the ratio of the mass of the model to the mass of the volume of the test medium contained in the right circular cylinder whose height is the model span and whose diameter is equal to the model chord. This volume is 0.1087 cubic foot. For the swept series the mass ratio is defined in the same manner except the volume of the test medium is now that which is contained in the conical frustrum whose height is equal to the model span and whose bases have diameters equal to the model root and tip chords, respectively. This volume is 0.1012 cubic foot.

Unswept Series

Experimental.- For a variety of configurations, past experience has shown that a frequently encountered variation of the altitude-stiffness parameter with Mach number is an almost linear increase to a high value near $M = 1$ and then, after a decrease, an increase again. Figure 4(a) shows that the unswept models exhibit this type of variation, but to a different degree for each model. All of these models exhibit essentially the same linear increase up to a Mach number of about 0.85. At this Mach number the values for the 10-percent-thick wing begin to deviate from those for the other wings. The Mach numbers at which the values for the 8- and 6-percent-thick models begin to differ from those of the 4-percent-thick model are about 0.88 and 0.91, respectively. As the figure shows, there is a marked difference between the flutter boundaries of the four models in both the magnitude of the usual high value of the parameter near $M = 1$ and in the Mach number at which this value occurs. There is a difference of approximately 10 percent between both the high value and the corresponding Mach number when the 4- and 10-percent-thick models are compared. Because of the close similarity between physical properties (see figs. 1 to 3 and table I) the differences in flutter boundaries must be primarily caused by aerodynamic effects of airfoil thickness.

Although there are no established analytical treatments of the effects of thickness on transonic flutter, it may be of interest to examine these experimental results in the light of what is known of transonic aerodynamics. Actually, there are very few data pertaining directly to transonic oscillatory aerodynamics; however, there is some evidence (refs. 1 and 4) that static aerodynamic characteristics may have some applicability in the flutter case, at least for the relatively low values

of reduced frequency encountered in the present investigation. Perhaps the most pertinent feature of transonic aerodynamics is the well established trend for thinner wings at moderate to high aspect ratios to exhibit higher slopes of the lift curve than do thick wings and the trend for thinner wings to experience smaller deviations in slope of the lift curve through the transonic speed range (refs. 5 and 6). Both of these characteristics are compatible with the observed flutter data shown in figure 4(a). In reference 6 it is pointed out through consideration of transonic similarity laws that wings having combinations of thickness and aspect ratio in the range of the present investigation would be expected to be subject to large effects of thickness and to large deviations in aerodynamic characteristics through the transonic range. These transonic similarity laws might be used as a basis for the conjecture that wings of lower aspect ratio would not be subject to as large an effect of thickness on the flutter characteristics as were the wings of the present investigation.

Also shown in figure 4(a) as a matter of interest are the data obtained for the flat plate having the same dimensions as the insert used in the airfoil models. The data for the flat plate do not follow the trends indicated by the data for the family of airfoil sections. It is difficult to assess the significance of this deviation of the data for the flat plate from the data for the family of circular-arc airfoil models. It might be expected that the data for the flat plate should fall at about the values extrapolated for a thickness ratio of 1.4 percent. The fact that the data for the flat plate do not follow this trend is probably caused by the change from a systematic variation of profile to the flat-sided, sharp-edged section of the flat-plate model.

Consideration of tunnel-wall effects.- A basis for applying corrections for wind-tunnel interference to oscillatory or flutter data for slotted-throat wind tunnels has not been established. However, the relatively large interference effects found for solid-throat tunnels (ref. 7) probably do not exist for slotted-throat tunnels.

Since the models did vary in thickness, there was some concern regarding possible tunnel blockage effects. Consequently, additional tests were made on both a 4- and a 10-percent-thick unswept model approximately one-half the size of the original models. These smaller models were so designed that their flutter parameters coincided with those of the original wings. Although the smaller wings behaved somewhat erratically, the data showed the same magnitude of thickness effect as indicated in figure 4(a) for the larger wings and coincided, within the limits of experimental error, with those of the larger wings. Consequently, tunnel blockage effects are believed not to have contributed any appreciable effect on the results from the original wings.

Comparison of experimental results with theory.- Flutter calculations using three uncoupled modes were made on the unswept series of wings. The results are presented and compared with experimental values in figure 5 where the altitude-stiffness parameter $\frac{b\omega_\alpha}{a}\sqrt{\mu}$ is plotted against Mach number.

Calculations for subsonic speeds were made by using both the linear compressible two-dimensional aerodynamic coefficients from reference 8 and the three-dimensional kernel function aerodynamics from reference 9. Calculations using the linear theory were made for all four unswept models. Calculations using the kernel function were made for only the 4-percent-thick wing. The linear theory predicted the upward curvature of the flutter boundary as Mach number increases. However, this theory predicted about a 15-percent higher value of the altitude-stiffness parameter than was found experimentally. This difference may be interpreted as the usual conservatism of two-dimensional theory at subsonic speeds. This conservatism agrees approximately with that found for similar wings by other investigators. (See ref. 10.) The three-dimensional-theory calculations showed excellent agreement with the experimental data up to Mach numbers where aerodynamic effects not included in the theory became pronounced.

The two-dimensional second-order theory of Van Dyke (ref. 11) was used in calculations for supersonic speeds at constant altitude. These calculations indicated that thicker models will require more stiffness to avoid flutter. The experimental evidence in the transonic range is the opposite; that is, thinner models required more stiffness to avoid flutter. However, the trend in the calculations is for the thickness effect to decrease as Mach number decreases toward one. Some indication exists for a crossover in the predicted flutter boundaries such that thinner models would be more susceptible to flutter as shown by the experiment. It should be noted that the Van Dyke second-order coefficients, as used herein, are expanded in powers of a frequency parameter and contain only terms through the cube of frequency.

As a matter of interest, flutter calculations using the linear two-dimensional aerodynamic theory of reference 12 were made at $M = 1.0$. The results of these calculations are presented in figure 6. Since the dynamic properties of all the wings are about the same, calculated flutter characteristics are nearly equal. It is interesting to note that an extrapolation of the experimental flutter data to zero thickness would yield much better agreement with the calculations which are, of course, based on thin-airfoil theory.

Swept Series

Initial tests of the swept models indicated very unusual flutter characteristics in that near $M = 1.0$ flutter occurred over a narrow band of Mach numbers at very low densities. When boundary-layer transition was fixed by applying narrow bands (approximately 6 percent of the local chord in width) of No. 60 carborundum grains 1/2 inch from the leading edge on both the upper and lower surfaces, this abnormal flutter behavior was eliminated. Consequently, all of the tests of the swept wings reported herein pertain to models having these transition strips installed. The range of Reynolds number, as indicated in table III(b) was from about 0.2×10^6 to 1.1×10^6.

L 2 0 3

Figure 4(b) shows the variation of the altitude-stiffness parameter with Mach number for the swept wings. These data exhibit a sharp drop near $M = 1.0$. This type of behavior has been observed for some delta wings (ref. 13) and appears to be associated with a change of flutter mode. In addition, the systematic decrease in the high value of the parameter as a function of increasing airfoil thickness found in the data for the unswept series does not appear here. The data for the 4-, 6-, and 8-percent-thick wings are in fair agreement, with each curve having a maximum value considerably less than that of the 2-percent-thick wing. Although these wings have variations in some of their properties, the mass-ratio parameter appears to have eliminated, to a great degree, the mass effects on the flutter boundaries as indicated by the agreement for all the models at Mach numbers below 0.90. This deduction seems reasonable since for high values of μ, as in this case, there is an approximate linear variation between model mass and the density required to produce flutter at a particular Mach number. As in the case of the unswept wings, the boundary for a typical aluminum-alloy insert is also included in the figure. As is seen from the figure, the agreement of the data for the flat plate with the data for the airfoil is poor at Mach numbers below $M = 1.00$. From the two-dimensional unsteady-airfoil data presented in reference 1 a more systematic effect of airfoil thickness would be expected than is indicated in figure 4(b), although the general trend seems to be consistent. Model dissimilarities and perhaps three-dimensional effects could be the cause, but no conclusion as to the latter can be drawn from the results of these tests.

CONCLUDING REMARKS

The transonic flutter characteristics of both a swept series and an unswept series of wings varying in airfoil thickness but having similar mass and stiffness properties have been experimentally determined. The tests indicate that for the range of variables covered, there is an appreciable aerodynamic effect of airfoil thickness for both swept and

unswept wings. In general, an increase in thickness has a stabilizing effect in that higher density is required to produce flutter at a given Mach number. This result is consistent with what would be expected from an examination of the steady-state aerodynamic characteristics of airfoils of different thicknesses.

Langley Research Center,
National Aeronautics and Space Administration,
Langley Field, Va., April 13, 1959.

REFERENCES

1. Wyss, John A., and Monfort, James C.: Effects of Airfoil Profile on the Two-Dimensional Flutter Derivatives for Wing Oscillating in Pitch at High Subsonic Speeds. NACA RM A54C24, 1954.

2. Hall, H., and Chapple, E. W.: The Aerodynamic Effects on Flutter of Wing Section and Thickness. Rep. No. Structures 207, British R.A.E., May 1956.

3. Herr, Robert W.: Preliminary Experimental Investigation of Flutter Characteristics of M and W Wings. NACA RM L51E31, 1951.

4. Yates, Carson E., Jr.: Calculation of Flutter Characteristics for Finite-Span Swept or Unswept Wings at Subsonic and Supersonic Speeds by a Modified Strip Analysis. NACA RM L57L10, 1958.

5. Fitzpatrick, J. E., and Rice, Janet B.: Aerodynamic Characteristics of Seventeen Airfoil Sections at Transonic Mach Numbers. Rep. R-25473-22 (Contract No. AF 33(038)-2209), United Aircraft Corp. Res. Dept., Apr. 30, 1953.

6. McDevitt, John B.: A Correlation by Means of Transonic Similarity Rules of Experimentally Determined Characteristics of a Series of Symmetrical and Cambered Wings of Rectangular Plan Form. NACA Rep. 1253, 1955. (Supersedes NACA RM A51L17b.)

7. Runyan, Harry L., Woolston, Donald S., and Rainey, A. Gerald: Theoretical and Experimental Investigation of the Effect of Tunnel Walls on the Forces on an Oscillating Airfoil in Two-Dimensional Subsonic Compressible Flow. NACA Rep. 1262, 1956. (Supersedes NACA TN 3416.)

8. Anon.: Tables of Aerodynamic Coefficients for an Oscillating Wing-Flap System in a Subsonic Compressible Flow. Rep. F.151, Nationaal Luchtvaartlaboratorium, Amsterdam, May 1954.

9. Watkins, Charles E., Woolston, Donald S., and Cunningham, Herbert J.: A Systematic Kernel Function Procedure for Determining Aerodynamic Forces on Oscillating or Steady Finite Wings at Subsonic Speeds. NASA TR R-48, 1959.

10. Widmayer, E., Jr., Lauten, W. T., Jr., and Clevenson, S. A.: Experimental Investigation of the Effect of Aspect Ratio and Mach Number on the Flutter of Cantilever Wings. NACA RM L50C15a, 1950.

11. Van Dyke, Milton D.: Supersonic Flow Past Oscillating Airfoils Including Nonlinear Thickness Effects. NACA Rep. 1183, 1954. (Supersedes NACA TN 2982.)

12. Nelson, Herbert C., and Berman, Julian H.: Calculations on the Forces and Moments for an Oscillating Wing-Aileron Combination in Two-Dimensional Potential Flow at Sonic Speed. NACA Rep. 1128, 1953. (Supersedes NACA TN 2590.)

13. Jones, George W., Jr., and Young, Lou S., Jr.: Transonic Flutter Investigation of Two 64° Delta Wings With Simulated Streamwise Rib and Orthogonal Spar Construction. NACA RM L56I27, 1957.

TABLE I.- MODEL PROPERTIES

(a) Unswept series

(Model elastic axis and center of gravity located at midchord)

Model	$\omega_{h,1}$	$g_{h,1}$	$\omega_{h,2}$	$g_{h,2}$	ω_α	g_α	m	m_l	I_α	EI	GJ
Flat-plate	94.9	0.0186	593.1	0.00658	529.7	0.00398	0.009957	0.0008658	0.0001307	1,068.9*	1,459.0*
4-percent-thick	87.3	------	563.0	-------	507.7	.00802	.01157	.001006	.0001520	1,050.2	1,601.0
6-percent-thick	89.8	.0242	564.2	.0112	505.2	.0102	.01182	.001028	.0001590	1,027.7	1,519.0
8-percent-thick	91.1	.0312	569.9	.0170	530.3	.0151	.01248	.001085	.0001607	1,247.0	1,750.0
10-percent-thick	93.6	.0264	561.7	.0198	508.3	.0165	.01261	.001097	.0001610	1,072.6	1,848.0

*Calculated values.

(b) Swept series

Model	$\omega_{h,1}$	$g_{h,1}$	$\omega_{h,2}$	$g_{h,1}$	ω_α	g_α	m
Flat-plate	145.8	0.00726	565.5	0.00922	906.7	0.00345	0.003752
2-percent-thick	148.3	.0142	512.7	.0151	808.2	.00963	.004438
4-percent-thick	137.6	.0271	524.6	.0259	807.4	.0194	.006298
6-percent-thick	135.9	.0378	500.8	.0353	760.3	.0266	.006121
8-percent-thick	131.1	.0508	495.7	.0550	760.0	.0529	.008087

TABLE II.- FIRST THREE NATURAL VIBRATION MODES FOR 2-PERCENT-THICK SWEPT MODEL

First mode

$(\omega_{h,1} = 148.3$ radians/sec$)$

Percent span	Percent chord				
	0	25	50	75	100
100.0	0.916	0.947	0.947	0.970	1.000
91.3	.794	.802	.824	.847	.878
82.7	.565	.649	.679	.687	.740
74.0	.420	.511	.557	.565	.626
65.3	.298	.359	.397	.489	.527
56.7	.191	.252	.324	.366	.382
48.0	.153	.206	.214	.260	.305
39.3	.107	.115	.176	.214	.244
30.7	.107	.137	.137	.160	.191
22.0	.137	.145	.130	.137	.153
13.3	.137	.107	.115	.122	.107

Second mode

$(\omega_{h,1} = 512.7$ radians/sec$)$

Percent span	Percent chord				
	0	25	50	75	100
100.0	0.601	0.719	0.797	0.876	1.000
91.3	.242	.379	.542	.660	.810
82.7	-.183	.065	.222	.434	.601
74.0	-.418	-.216	-.052	.209	.418
65.3	-.529	-.373	-.190	.608	.275
56.7	-.529	-.431	-.301	-.092	.150
48.0	-.425	-.412	-.314	-.144	.072
39.3	-.301	-.320	-.275	-.170	.046
30.7	-.222	-.222	-.203	-.157	-.072
22.0	-.118	-.144	-.163	-.144	-.092
13.3	-.098	-.072	-.072	-.072	-.072

Third mode

$(\omega_{\alpha} = 808.2$ radians/sec$)$

Percent span	Percent chord				
	0	25	50	75	100
100.0	1.000	0.969	0.878	0.832	0.787
91.3	.752	.650	.593	.479	.331
82.7	.502	.400	.262	.114	-.205
74.0	.456	.251	.103	-.251	-.502
65.3	.422	.194	-.160	-.422	-.775
56.7	.467	.228	-.148	-.467	-.878
48.0	.445	.274	-.057	-.479	-.912
39.3	.365	.274	.057	-.342	-.821
30.7	.331	.239	.080	-.239	-.673
22.0	.160	.182	.137	-.182	-.422
13.3	.103	.103	.080	-.068	-.217

TABLE III.- BASIC TEST DATA

(a) Unswept series

Model	M	a	ρ	q	R	ω_f	k_f	μ	$\frac{b\omega_a}{a}\sqrt{\mu}$
Flat-plate	0.714	512	2.662×10^{-3}	180.6	1.380×10^{6}	240.0	0.125	34.81	1.16
	.804	512	2.011	174.6	1.175	241.9	.112	52.85	1.43
	.846	511	1.769	168.0	1.086	233.7	.103	51.98	1.42
	.868	510	1.580	157.0	.993	231.2	.099	57.76	1.50
	.916	507	1.351	148.6	.893	181.6	.074	67.73	1.63
	.926	508	1.293	145.8	.865	172.8	.070	71.06	1.67
	.960	513	1.318	162.7	.917	-----	.046	69.06	1.63
	.965	510	1.498	184.3	1.047	188.5	.052	60.84	1.54
	1.008	511	1.592	214.9	1.163	202.9	.058	57.30	1.49
	1.064	508	1.635	244.3	1.258	169.6	.063	55.80	1.48
4-percent-thick	0.756	514	2.375×10^{-3}	182.9	1.304×10^{6}	209.2	0.102	44.36	1.25
	.801	513	2.030	175.4	1.179	204.8	.095	52.27	1.36
	.856	511	1.664	162.4	1.031	184.1	.080	64.00	1.51
	.880	514	1.465	152.1	.935	175.3	.074	72.76	1.60
	.904	507	1.406	151.0	.915	165.2	.069	75.17	1.65
	.930	508	1.329	151.8	.891	147.7	.059	80.10	1.70
	.967	511	1.361	169.3	.952	149.5	.058	78.32	1.67
	1.030	506	1.310	181.5	.974	157.1	.057	81.36	1.72
	1.066	511	1.197	182.3	.923	154.6	.054	88.92	1.78
	1.102	505	1.111	175.4	.883	143.8	.049	95.84	1.87
	1.104	507	1.069	170.8	.851	138.2	.047	98.60	1.89
6-percent-thick	0.715	510	2.971×10^{-3}	201.1	1.542×10^{6}	221.8	0.116	36.72	1.14
	.718	509	2.988	202.9	1.556	224.9	.117	36.60	1.14
	.795	508	2.191	181.6	1.262	197.3	.093	49.56	1.33
	.814	506	2.184	188.7	1.285	198.5	.092	49.87	1.34
	.836	512	1.851	172.6	1.119	191.6	.085	58.98	1.44
	.851	509	1.859	177.4	1.144	184.7	.081	58.37	1.44
	.905	511	1.580	171.6	1.035	155.2	.064	68.06	1.55
	.907	512	1.623	178.1	1.065	158.3	.065	66.59	1.53
	.913	512	1.440	161.6	.951	150.8	.061	74.65	1.62
	.923	517	1.458	169.1	.967	177.2	.071	74.30	1.60
	.927	512	1.418	163.2	.951	154.6	.062	76.56	1.64
	.956	510	1.738	209.4	1.204	188.5	.073	61.78	1.48
	1.017	506	1.848	249.5	.643	211.7	.078	59.29	1.46
8-percent-thick	0.745	512	2.857×10^{-3}	161.6	1.538×10^{6}	150.8	0.075	38.44	1.22
	.848	509	2.138	178.1	1.313	158.3	.070	53.73	1.45
	.886	506	1.807	202.9	1.154	221.8	.095	63.84	1.59
	.913	507	1.731	201.1	1.141	224.9	.091	63.20	1.58
	.932	508	1.768	171.6	1.192	155.2	.062	65.12	1.60
	.954	510	2.009	172.6	1.388	191.6	.075	57.61	1.50
	.975	510	2.431	163.2	1.721	154.6	.059	47.33	1.36
	1.008	509	2.460	169.1	1.798	177.2	.066	46.51	1.35
10-percent-thick	0.741	514	2.782×10^{-3}	206.5	1.486×10^{6}	213.6	0.107	41.47	1.21
	.808	512	2.119	185.0	1.241	186.0	.085	53.58	1.38
	.864	512	1.751	174.1	1.097	178.4	.077	64.96	1.52
	.881	512	1.701	175.7	1.086	166.5	.070	66.59	1.54
	.915	512	1.706	190.3	1.131	-----	-----	65.77	1.53
	.951	512	1.947	234.9	1.342	194.8	.076	58.22	1.44
	.976	512	2.361	298.4	1.675	201.7	.077	48.30	1.31

L-203

[redacted]

TABLE III.- BASIC TEST DATA - Concluded

(b) Swept series

Model	M	a	ρ	q	R	ω_f	k_f	μ	$\frac{b\omega_a}{a}\sqrt{\mu}$
Flat-plate	0.734	512	1.521×10^{-3}	109.5	0.553×10^{6}	503.2	0.174	23.91	1.13
	.818	511	1.445	128.2	.586	360.9	.112	25.60	1.17
	.820	511	1.225	111.5	.501	-----	-----	30.25	1.27
	.887	508	1.172	121.2	.514	313.7	.091	31.25	1.30
	.923	507	1.037	115.7	.473	313.7	.087	35.16	1.38
	.952	507	.8181	96.9	.385	292.9	.079	44.89	1.56
	.967	505	.7098	86.2	.340	272.9	.073	51.70	1.68
	.974	506	.6006	74.3	.291	251.2	.066	60.84	1.82
	.980	510	.5314	66.3	.260	251.2	.065	68.72	1.92
	1.004	510	.4352	58.1	.218	230.3	.058	84.64	2.13
	1.026	510	.3805	53.0	.195	220.3	.055	96.24	2.27
	1.040	509	.4225	61.0	.221	230.3	.056	86.68	2.16
	1.044	509	.3656	54.3	.195	220.3	.053	100.00	2.32
	1.064	510	.4788	71.0	.354	238.5	.057	76.91	2.03
	1.067	508	.8385	124.9	.444	292.9	.070	43.96	1.54
	1.068	505	.5615	82.5	.298	251.2	.061	65.29	1.89
	1.069	507	.7473	111.3	.396	282.9	.068	49.00	1.63
	1.074	505	.6540	97.5	.349	272.0	.065	56.10	1.75
	1.101	504	.9113	142.6	.500	-----	-----	40.45	1.49
	1.103	504	.9981	156.7	.545	339.1	.079	36.72	1.42
2-percent-thick	0.741	506	1.480×10^{-3}	103.9	0.542×10^{6}	348.3	0.121	28.51	1.11
	.844	505	1.124	102.1	.472	314.4	.096	37.70	1.28
	.901	505	.8455	89.6	.389	294.2	.084	48.44	1.45
	.951	507	.6225	72.4	.296	257.0	.069	67.90	1.71
	.997	511	.4015	52.1	.410	222.3	.057	105.06	2.11
	1.002	514	.4019	53.3	.413	224.7	.057	115.56	2.10
	1.038	506	.5854	80.7	.304	257.0	.064	71.57	1.76
	1.043	505	.7713	106.0	.401	280.4	.070	54.91	1.55
	1.057	504	.9513	135.1	.499	330.6	.081	44.36	1.39
	1.104	500	1.139	173.4	.625	353.2	.083	36.97	1.28
4-percent-thick	0.754	502	2.032×10^{-3}	145.4	0.759×10^{6}	344.0	0.118	29.59	1.14
	.818	503	1.689	142.9	.687	322.2	.102	35.76	1.25
	.875	503	1.381	133.9	.604	302.0	.089	39.31	1.31
	.915	503	1.117	118.2	.512	275.3	.078	53.58	1.53
	.944	505	.8723	99.1	.413	251.1	.068	69.06	1.73
	.978	504	1.531	186.0	.744	314.1	.083	38.81	1.30
	.979	507	.8518	104.8	.417	251.1	.066	70.39	1.74
	.981	506	.8327	102.7	.410	251.1	.066	72.59	1.77
	.982	504	1.066	130.5	.523	267.2	.070	56.70	1.57
	.988	504	1.269	157.4	.626	295.5	.077	24.90	1.04
	.992	502	1.719	213.1	.847	365.8	.096	35.05	1.24
	1.011	500	1.907	243.6	.951	377.9	.097	31.47	1.18
	1.045	500	2.118	289.3	1.096	417.4	.104	28.47	1.12
6-percent-thick	0.854	504	1.408×10^{-3}	130.4	0.597×10^{6}	288.9	0.087	43.16	1.29
	.904	506	1.132	118.4	.509	266.1	.076	53.44	1.43
	.937	506	.8930	100.4	.417	241.8	.066	67.73	1.61
	.970	508	.6450	78.3	.313	427.3	.113	94.09	1.89
	.977	508	.6520	80.4	.318	219.0	.057	93.12	1.88
	.985	512	.6500	82.6	.321	226.6	.059	93.51	1.87
	.987	502	1.280	157.0	.626	277.5	.073	47.61	1.36
	.990	506	1.062	133.3	.523	263.8	.069	57.30	1.48
	.990	508	.8560	108.3	.422	238.7	.062	70.90	1.64
	1.016	500	2.220	288.7	1.115	396.1	.101	27.04	1.03
	1.023	501	1.596	209.6	.810	349.7	.089	38.07	1.22
8-percent-thick	0.714	512	2.701×10^{-3}	180.4	0.956×10^{6}	297.9	0.106	29.48	1.05
	.776	513	2.083	165.2	.803	317.7	.104	38.07	1.19
	.847	513	1.735	163.6	.728	270.6	.081	46.10	1.31
	.866	511	1.589	155.6	.685	266.8	.079	49.98	1.37
	.892	510	1.428	147.4	.632	-----	-----	55.80	1.45
	.906	508	1.307	138.3	.591	239.4	.068	60.84	1.52
	.935	512	1.049	120.3	.490	232.6	.063	76.39	1.69
	.956	512	.9900	118.5	.473	221.2	.059	81.00	1.74
	.994	510	1.223	157.2	.606	-----	-----	65.45	1.57
	1.001	511	1.316	172.2	.655	249.3	.063	60.84	1.61
	1.008	512	1.429	190.1	.715	251.6	.064	55.50	1.44
	1.013	513	1.706	238.2	.886	270.6	.068	45.43	1.30

[redacted]

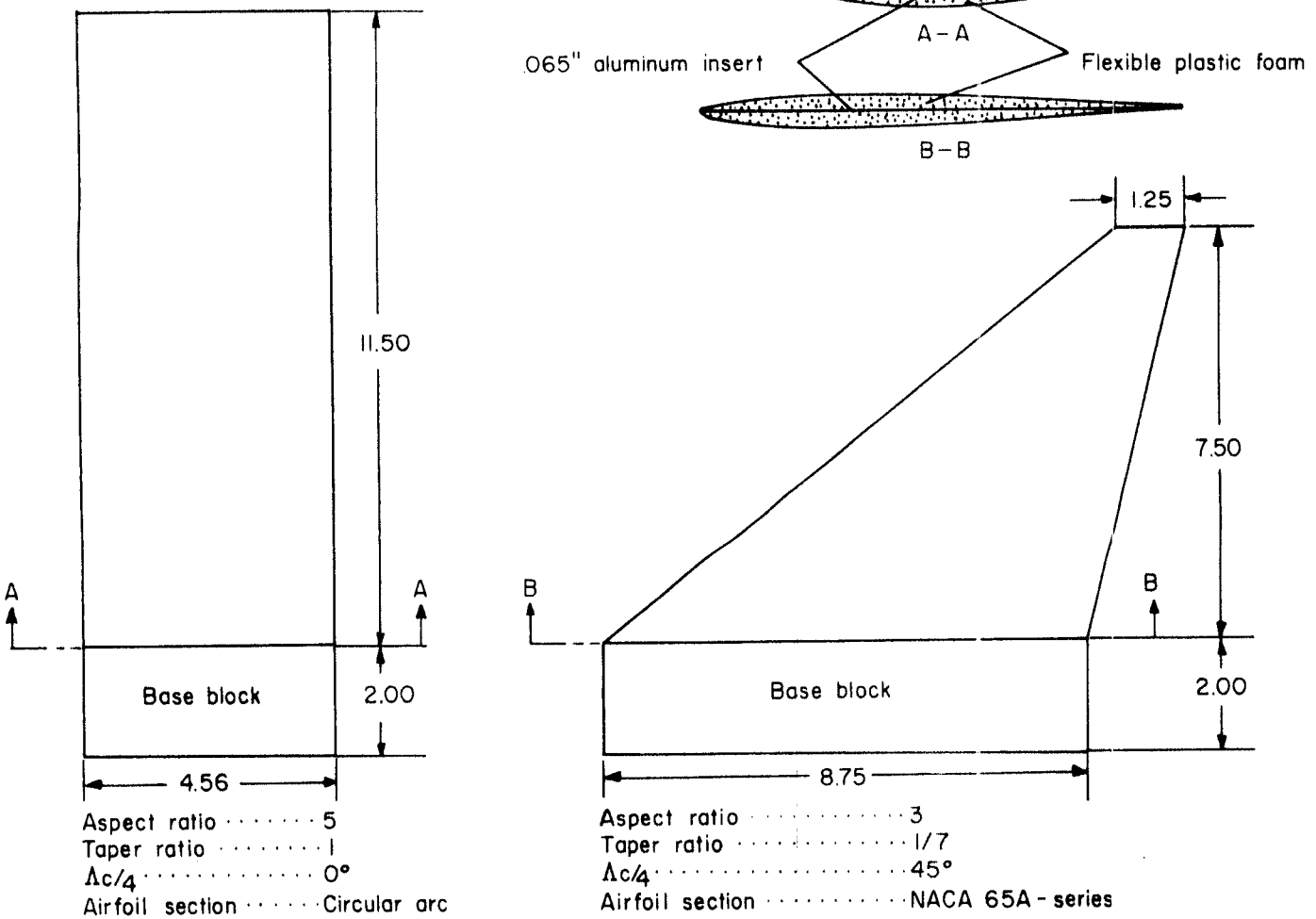

(a) Unswept series.

(b) Swept series.

Figure 1.- Line drawings of models with pertinent dimensions in inches.

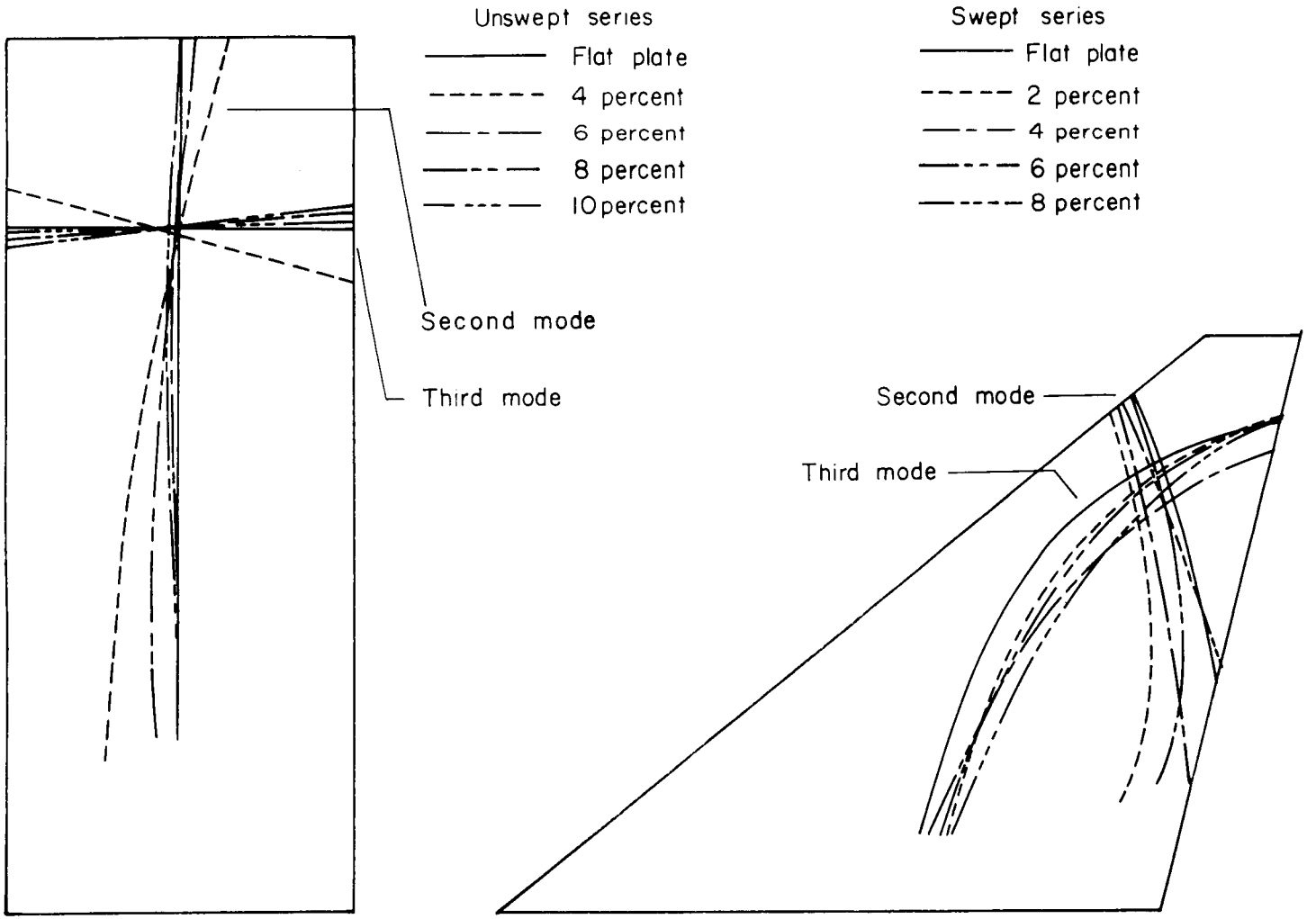

(a) Unswept series.

(b) Swept series.

Figure 2.- Node lines for second and third natural modes.

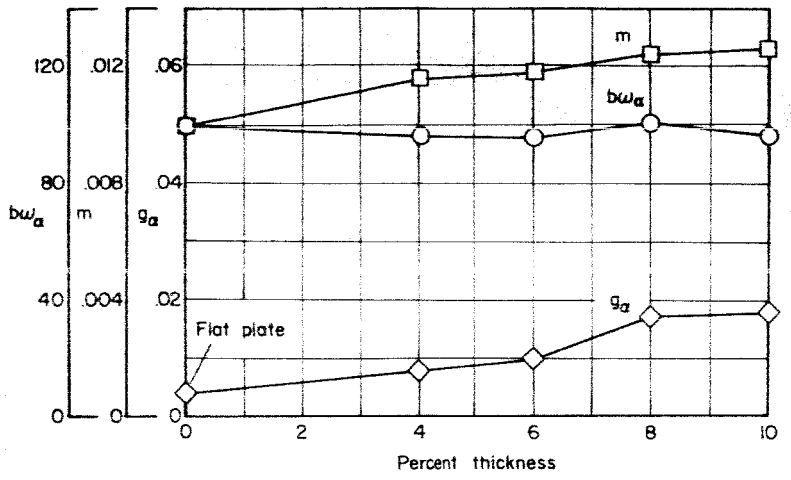

(a) Unswept series.

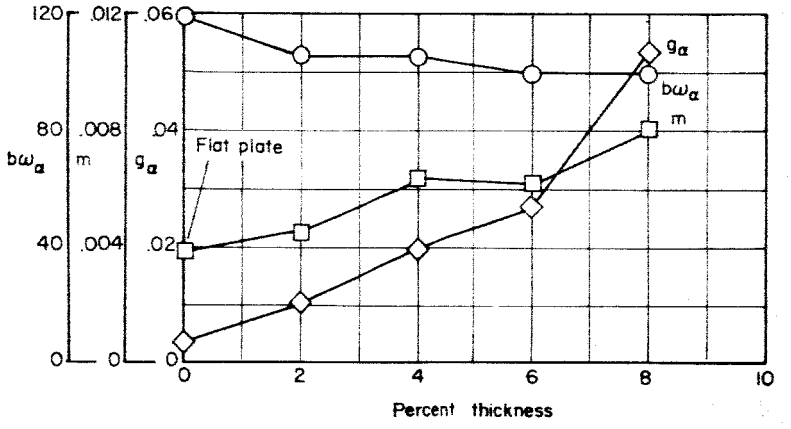

(b) Swept series.

Figure 3.- Selected model properties.

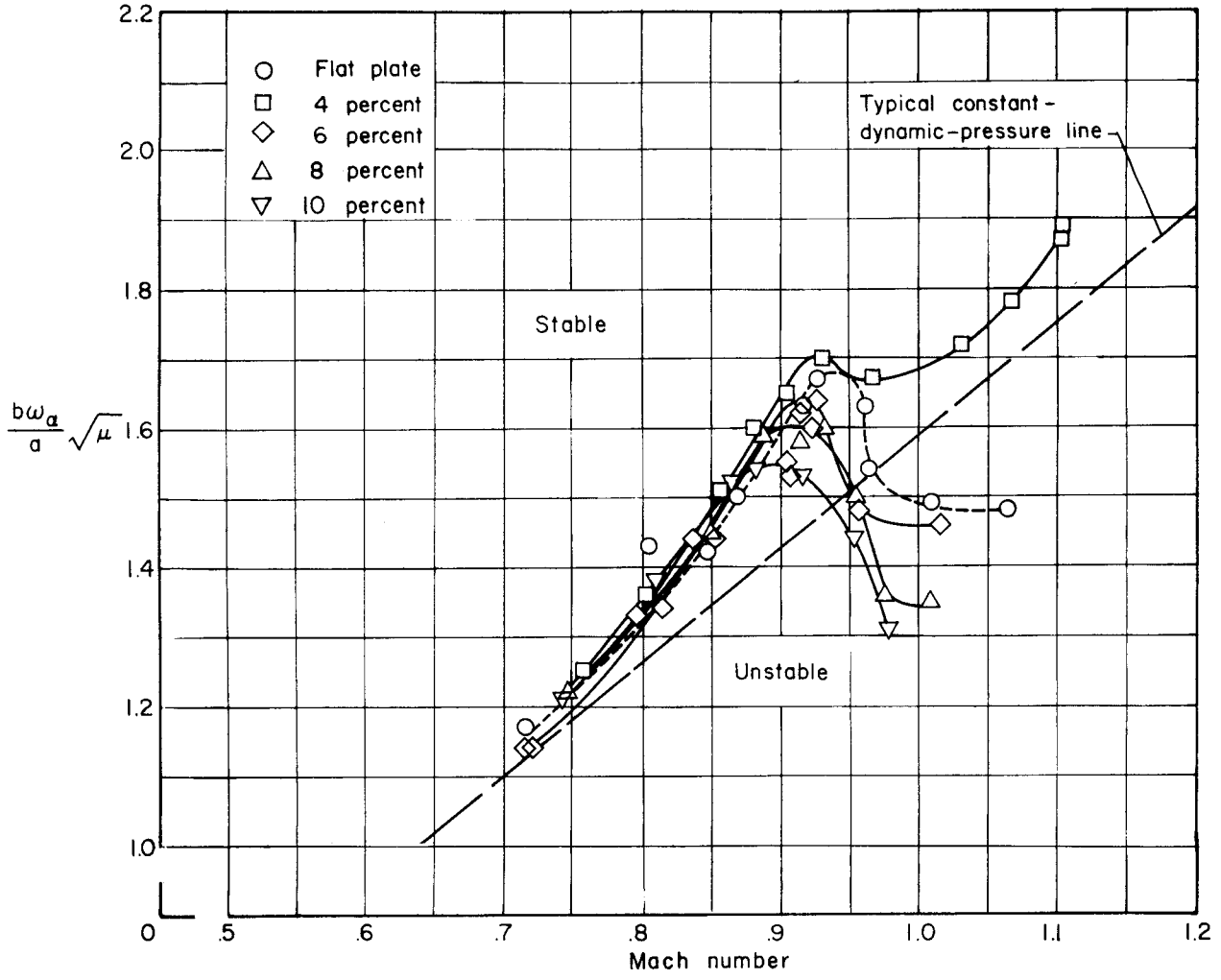

(a) Unswept series.

Figure 4.- Variation of altitude-stiffness parameter with Mach number.

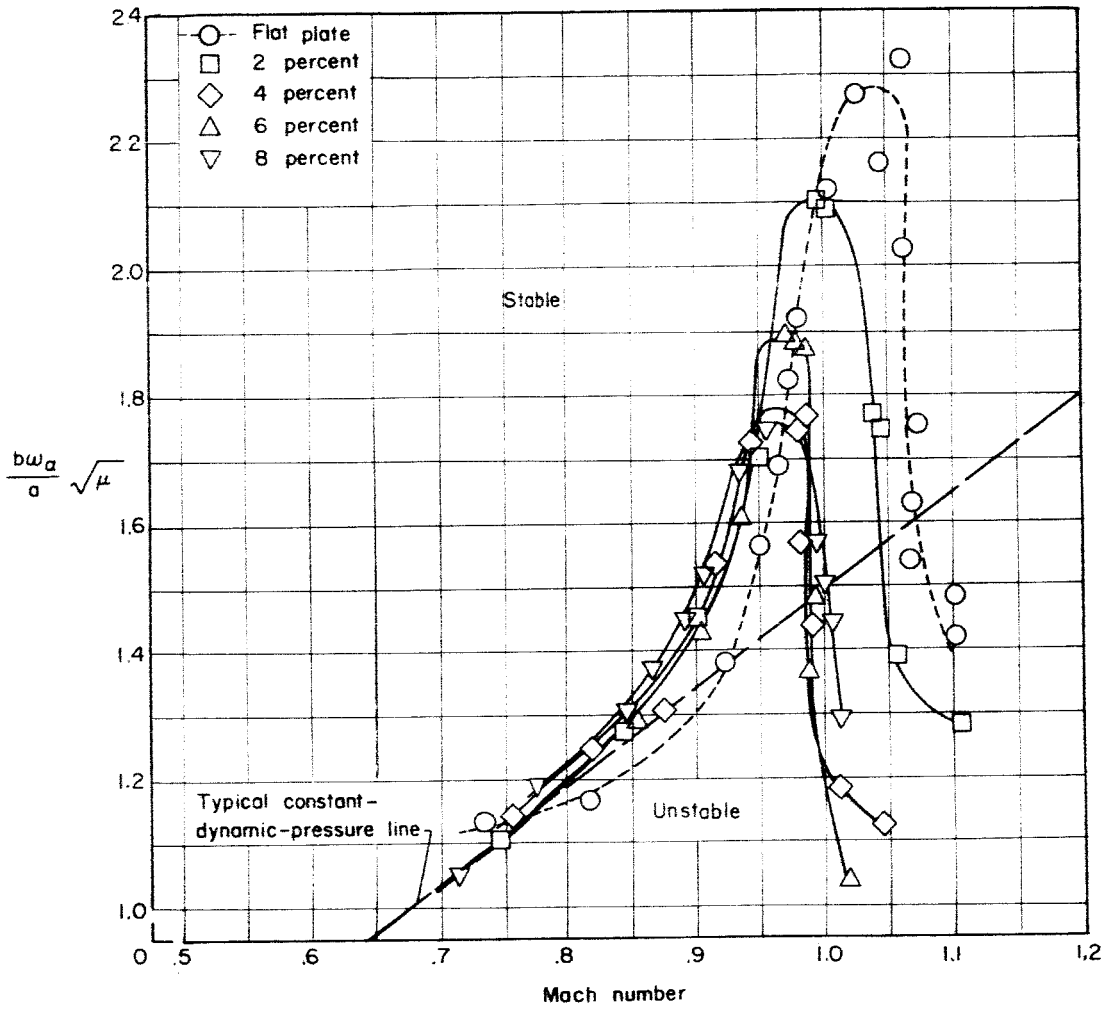

(b) Swept series.

Figure 4.- Concluded.

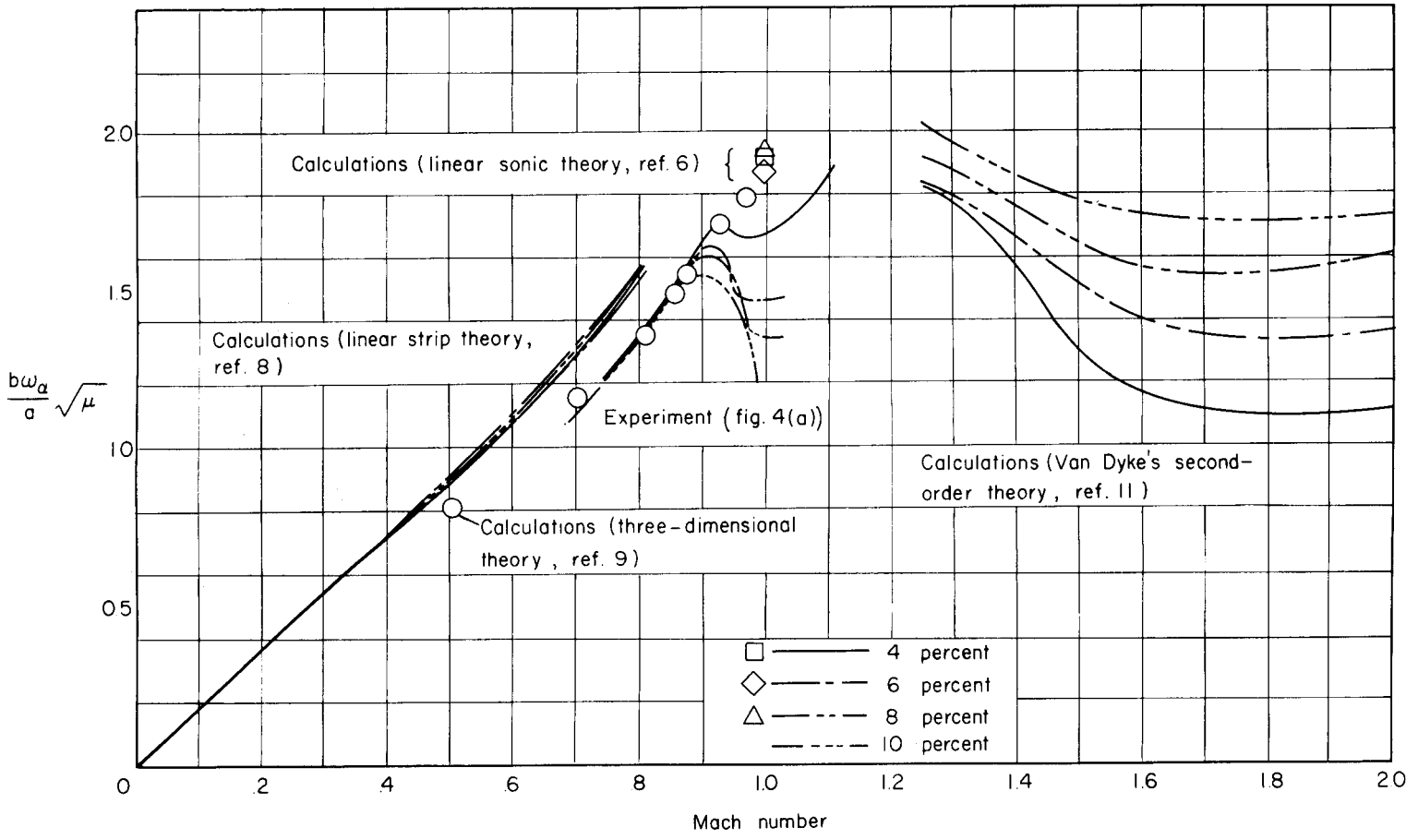

Figure 5.- Comparison of experimental values with theoretical values of altitude-stiffness parameter for the unswept wings at various Mach numbers. (Experimental values of density were used in making calculations for subsonic and sonic speeds. A constant density of 0.0018 slug/cu ft was used in making calculations for supersonic speeds.)

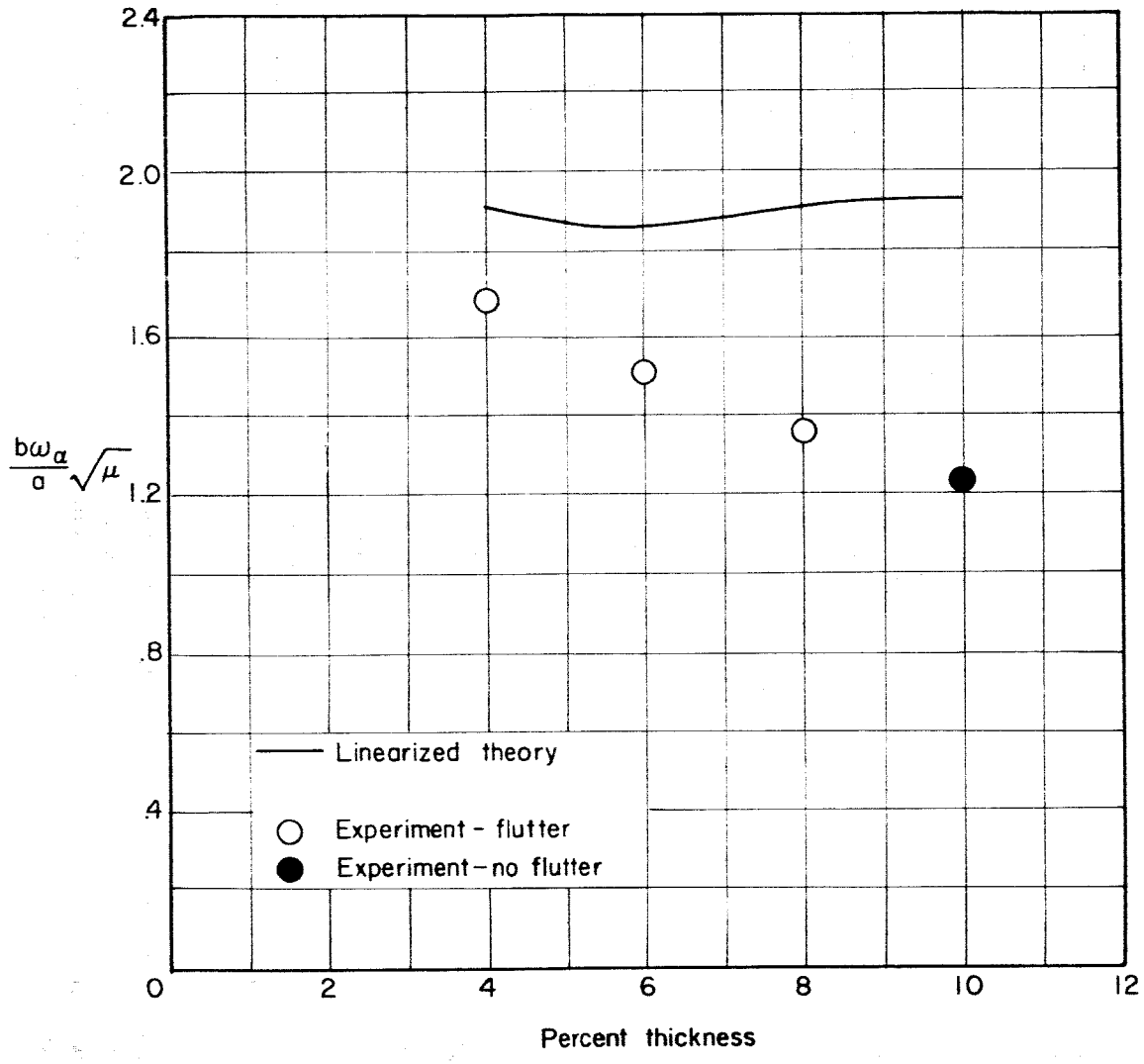

Figure 6.- Comparison of experimental values with theoretical values of altitude-stiffness parameter for the unswept wings at a Mach number of 1.0.